Enantioselective Catalysis Hot Paper

Deutsche Ausgabe: DOI: 10.1002/ange.201603072
Internationale Ausgabe: DOI: 10.1002/anie.201603072

Radical Changes in Lewis Acid Catalysis: Matching Metal and Substrate

*Tim Bleith[+], Qing-Hai Deng[+], Hubert Wadepohl, and Lutz H. Gade**

Abstract: *Whereas the stereochemical rigidity of the coordination sphere of boxmi/Cu^{II} catalysts is key to achieving high enantioselectivity in the electrophilic alkylation of β-ketoesters, this pathway is outperformed by a radical process for the corresponding catalytic transformation of oxindoles, giving rise to racemic products. For the corresponding Zn^{II} catalysts, the selectivity in the latter process is outstanding despite the greater plasticity of the coordination shell. This reaction was thus developed into a highly useful synthetic method, which enabled the conversion of wide range of substrates with high yields and enantioselectivities.*

In molecular catalysis, the choice of the metal center may have a dramatic effect on the reactivity, chemo-, and stereoselectivity of the reaction of interest.[1–3] In principle, this can be traced back to preferred coordination geometries associated with the (open or closed) valence shells, the accessibility of different metal redox states in a given coordination environment, as well as possible metal–substrate interactions. Whereas each of these factors may be well understood, their interplay is less so and frequently difficult to predict. Screening metal ions of a given oxidation state is therefore a routine exercise in the search and optimization of new catalysts, in particular in enantioselective Lewis acid catalysis.

Copper[4,5] and zinc,[6,7] giving rise to analogous molecular catalysts, are d block metals commonly tested and employed in this context and frequently display different reactivity.[8–15] However, with the exception of a few examples of stereoselectivity reversal,[11–14,16] their different catalytic behaviors have received little attention.

Herein, we report the mechanistic basis for the apparent disparity observed for the behavior of the two metals in the Lewis acid catalyzed enantioselective alkylation of two closely related substrates, cyclic β-ketoesters and 3-substituted oxindoles, which may be viewed as paradigmatic for the challenges incurred in this field of catalyst development. The 3,3-disubstituted oxindole motif, in particular, has attracted considerable attention,[17–21] as it occurs in a variety of biologically and pharmacologically active compounds.[22–25] Most published enantioselective syntheses employ noble metals,[17–19,26–31] whereas 3d transition-metal-catalyzed[32] as well as organocatalytic[33–36] methods have been recently introduced.

Our study was initiated by the unexpected observation that the enantioselective alkylation of *N*-Boc oxindoles with boxmi/Cu^{II} catalysts yielded the target product as a racemic mixture, whereas high enantioselectivity was observed using Zn^{II} catalysts (see Figure 1). This contrasted with the previous observation that the structurally related cyclic β-ketoesters could be converted with high selectivity using copper(II)-based catalysts whereas zinc(II) catalysts led to diminished selectivity.[37–40]

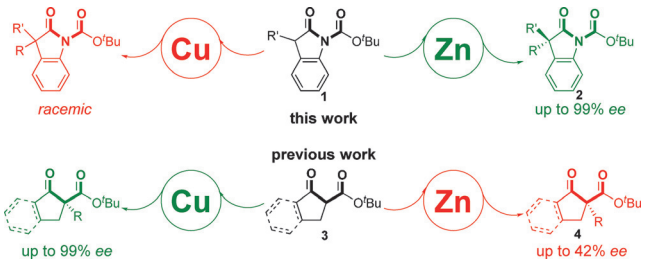

Figure 1. Schematic representation of the differences found for copper and zinc catalysts in the alkylation of oxindoles and β-ketoesters.[41]

The drastic difference between high enantioselectivity and racemate formation observed for the oxindole substrates suggested the operation of two different mechanistic pathways rather than competition between two activation barriers in the same catalytic cycle, which may operate in the alkylation of the β-ketoesters. To elucidate the underlying reasons, the key steps were carried out stoichiometrically with both metals. First, the zinc enolate complex **5** was synthesized by the reaction of $ZnEt_2$ with boxmiH-Ph and subsequent addition of oxindole **1e** (Scheme 1, top). Its further conversion with allyl bromide yielded **2ea** with high stereoselectivity (98% *ee*) and was found to be first order with respect to the concentration of **5** as well as the concentration of allyl bromide ($k = 4.1(6) \times 10^{-4}$ L mol^{-1} s^{-1}; see also the Supporting Information). The same rate law was found for the conditions of the catalytic process and supports the assumption that the rate- and selectivity-determining step is an S_N2 process.

The preference for *Si* face attack for the (*S*,*S*)-configured ligand was confirmed by X-ray structure analysis of **2am** (see the Supporting Information). In situ NMR studies of the

[*] T. Bleith,[+] Dr. Q.-H. Deng,[+] Prof. H. Wadepohl, Prof. L. H. Gade
Anorganisch-Chemisches Institut, Universität Heidelberg
Im Neuenheimer Feld 270, 69120 Heidelberg (Germany)
E-mail: lutz.gade@uni-hd.de
Dr. Q.-H. Deng[+]
Present Address: The Education Ministry Key Lab of Resource Chemistry and Shanghai Key Laboratory of Rare Earth Functional Materials, Shanghai Normal University
Shanghai 200234 (P.R. China)
[+] These authors contributed equally to this work.

Supporting information for this article can be found under: http://dx.doi.org/10.1002/anie.201603072.

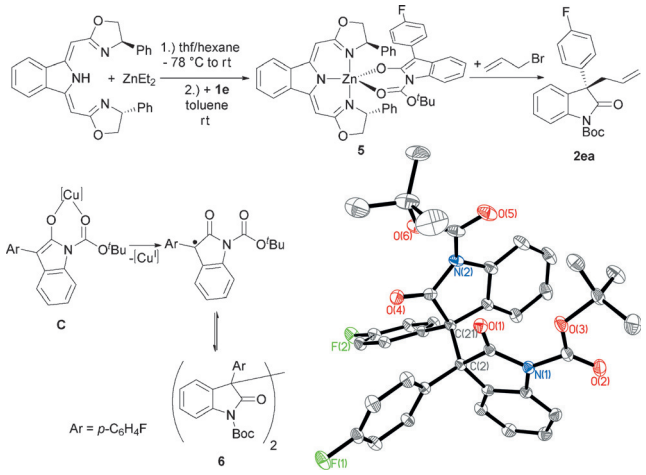

Scheme 1. Top: Synthesis of **5** and subsequent conversion into **2ea**. Bottom: Radical sequence leading to the oxindole dimer **6** and its molecular structure in the solid state (hydrogen atoms omitted for clarity). C(2)–C(21) 1.6097(18) Å.

catalytic reaction also established complex **5** as the resting state of the catalyst, and compound **5** was found to be catalytically active (see the Supporting Information for further details). These observations are consistent with a mechanistic proposal in which coordination (see Scheme 2, step I) and deprotonation of the oxindole (step II) occur first, followed by the S_N2-type allylation (step III) and subsequent dissociation of the product (step IV).

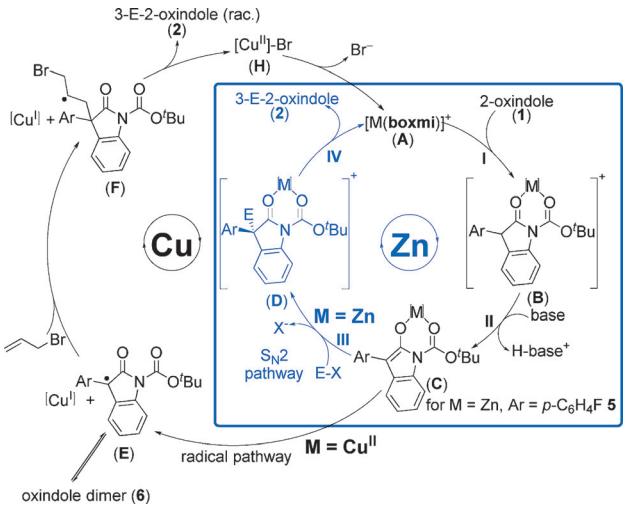

Scheme 2. Proposed mechanistic cycle for the copper- and zinc-catalyzed allylation of oxindoles.

On the other hand, with boxmi/Cu^{II} complexes as substoichiometric or stoichiometric reagents, the racemic allylation product was observed along with the temporary formation of approximately 20% of the oxindole dimer **6** (Scheme 1, bottom; see the Supporting Information details). Notably, Cu^{I} salts were able to convert this dimer into the respective allylated oxindole in a racemic fashion. These findings were taken as evidence for a radical reaction pathway that is not accessible under zinc catalysis. Furthermore, DFT potential energy surface scans of the Cu–oxindole bonds in **C** indicate a low-energy homolytic dissociation pathway that is inaccessible with the redox-robust Zn analogues (see the Supporting Information).

The radical pathway is kinetically favored over the S_N2 allylation within the coordination sphere (step III in Scheme 2). Following this homolytic cleavage of the coordinative bond yielding a Cu^{I} complex and an oxindole radical (intermediate **E**), a radical reaction with allyl bromide takes place, leading to the racemic product. The bromine radical formed in this reaction step may either oxidize a Cu^{I} complex to a Cu^{II} complex, closing the copper-catalyzed mechanistic cycle, or abstract a hydrogen atom from an oxindole, starting a radical-chain mechanism, rendering the copper complexes initiators of the reaction. Such processes are not unprecedented as Cu^{II} salts and complexes are well known as atom transfer radical (ATR) reagents in radical couplings, cyclizations,[42–45] or polymerizations (ATRP).[42,46] This leads to an extended mechanistic proposal for this reaction manifold as depicted in Scheme 2.

DFT modeling of step III in Scheme 2 showed that the Zn complexes have a flexible coordination environment, rendering a trigonal-bipyramidal as well as a square-pyramidal coordination geometry energetically accessible (see the Supporting Information for details). The transition states originating from both stereoisomers were calculated and are depicted in Figure 2. The *Si* face attack starting from the square-pyramidal geometry was found to have the lowest activation barrier, which is consistent with the configuration of the products, which was derived from the X-ray structure of **2am** (see the Supporting Information).

In contrast to the alkylation of oxindoles, the ester enolates generated in the alkylation of β-ketoesters are

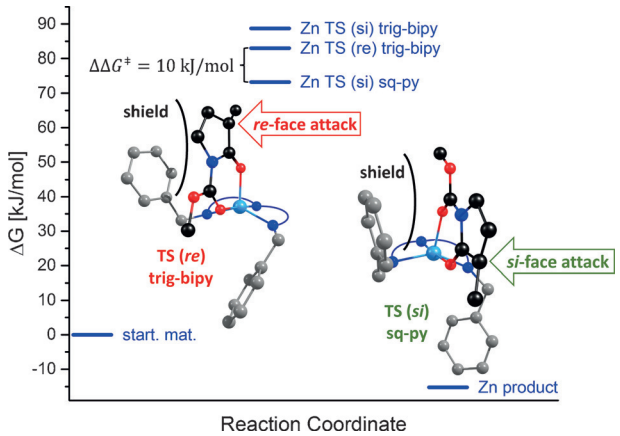

Figure 2. Transition states for the enantioselective allylation of [Zn(boxmi)(**1**-H)] with allyl bromide calculated at the B3LYP/def2-SVP//B3LYP/def2-QZVPP/COSMO level of theory. sq-py = square-pyramidal, trig-bipy = trigonal-bipyramidal. A simplified model of the reactive center is also shown; the phenyl substituents of the boxmi ligand are shown in gray.

redox-stable, as cyclovoltammetric measurements established oxidation potentials for the enolates of 0.1 V vs. SCE for the oxindoles and 0.8 V for the β-ketoesters (see the Supporting Information). The mechanism for this transformation is similar to that of the alkylation of oxindoles (see Scheme 2), but without intervening radical reactivity.[41] Thus both copper and zinc complexes were found to act as chiral Lewis acid catalysts, with the copper-based systems outperforming the zinc-based catalysts (99 vs. 42% *ee*).

This difference in enantioselectivity was thought to be related to differences in the structures and reactivities of the Cu and Zn ester enolates. The reaction with allyl bromide (step III in Scheme 2) was modeled by DFT calculations (see Scheme 3). A relaxed potential energy surface scan of the

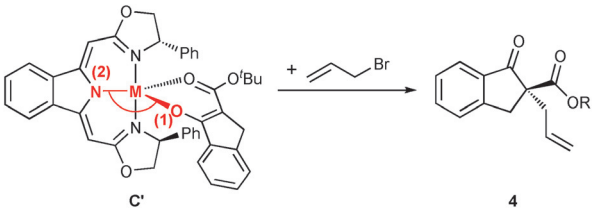

Scheme 3. Allylation of β-ketoesters. M = Zn or Cu.

N(2)-M-O(1) angle in the substrate enolate complexes **C′** revealed a high plasticity of the coordination sphere of the zinc complexes whereas the copper complexes were characterized by a greater stereochemical rigidity of their coordination environment (see Figure 3). Whereas for the Cu^{II} complexes, the optimal geometry is square-pyramidal ($\measuredangle$(N(2)-Cu-O(1)) = 168°), the corresponding Zn complexes feature two local structural minima ($\measuredangle$(N(2)-Zn-O(1)) = 165° and $\measuredangle$(N(2)-Zn-O(1)) = 110°, representing a trigonal-bipyramidal conformation) separated by a low activation barrier ($\Delta E^{+} = 11$ kJ mol^{-1}). The N(2)-Zn-O(1) angle determines the accessibility of the reactive carbon atom for the nucleophilic substitution (see Figure 4).

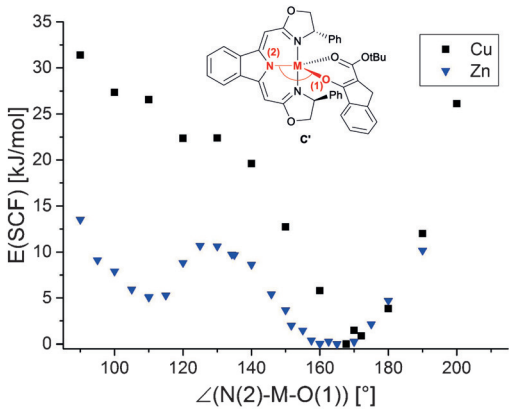

Figure 3. Relaxed potential energy surface scan (D3-B3LYP/def2-TZVPP/def2-SVP) of [M(boxmi)(**3**-H)] (**C′**) complexes along the N(2)-M-O(1) angle. Images of structural arrangements, including possible reaction trajectories of both minimum-energy conformers, are included in the Supporting Information.

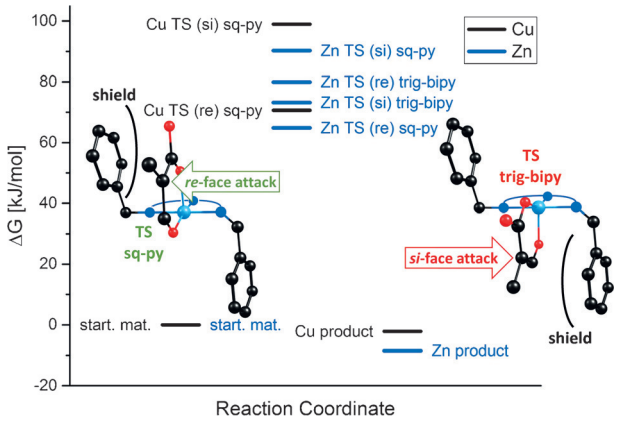

Figure 4. Transition states for the enantioselective allylation of [M(boxmi)(**3**-H)] with allyl bromide. Calculated at the B3LYP/def2-SVP//B3LYP/def2-QZVPP/COSMO level of theory. sq-py = square-pyramidal, trig-bipy = trigonal-bipyramidal. A simplified model of the reactive center is also shown.

The energies of the transition states for the alkylation of β-ketoesters are shown in Figure 4. The transition states for Cu and Zn complexes with the same configuration are very similar in energy (*Re*: $\Delta G^{+} = 71$ and 65 kJ mol^{-1}; *Si*: $\Delta G^{+} = 99$ and 90 kJ mol^{-1}, respectively). The experimentally observed preference for *Re* face attack[41] was also confirmed by these modeling studies. Owing to the additional transition states for Zn that result from the trigonal-bipyramidal conformer, a *Si* face attack is accessible at 73 kJ mol^{-1}. Therefore, the use of zinc complexes for the alkylation of β-ketoesters results in significantly reduced stereodiscrimination for this class of substrates (42% *ee* vs. 99% *ee*),[41] which can be attributed to the high plasticity of its coordination sphere.

The analysis of the geometries and transition states reveals that the stereochemical rigidity of the coordination sphere for the Cu catalysts (a consequence of the open d shell) is key for the selective transformation of β-ketoesters, and the coordination plasticity of the analogous Zn complexes hampers their ability to perform highly selective transformations. Indeed, for the catalytic transformation of oxindoles, the conformational rigidity of Cu^{II} would also be beneficial; however, the reaction at the metal center is outperformed by a radical reaction that does not take place within the chiral space created by the stereodirecting ligand. In the case of Zn, the selectivity for the alkylation of oxindoles is outstanding despite the greater flexibility of the coordination shell.

The zinc-catalyzed enantioselective alkylation of oxindoles was also further developed as a synthetic method. Alkylating N-Boc-protected 3-aryl oxindoles using allyl bromide under basic conditions generated the corresponding 3,3′-disubstited oxindoles in high yields (84–91%) with excellent enantioselectivities (94–99% *ee*) regardless of the nature of the substituents at the oxindole framework (**2aa**–**2la**; Scheme 4).

Finally, we investigated various alkylating reagents (Scheme 5). Treating 3-phenyloxindole **1a** with differently substituted allyl or benzyl bromides yielded the desired

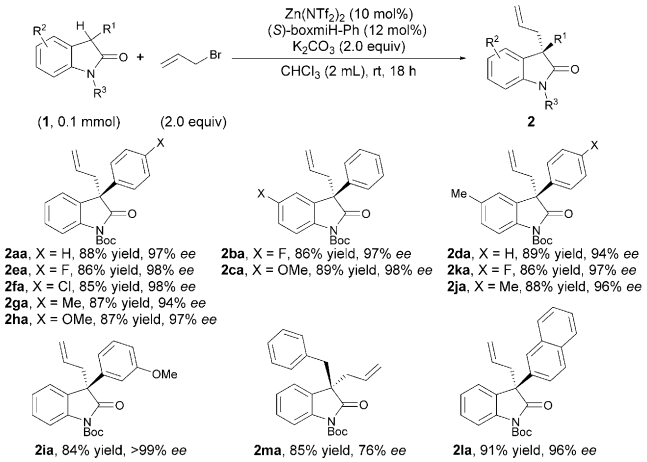

Scheme 4. Enantioselective allylation of oxindole derivatives with allyl bromide. Yields refer to isolated products; the *ee* values were determined by HPLC analysis on a chiral stationary phase. For the optimization of the reaction conditions, see the Supporting Information.

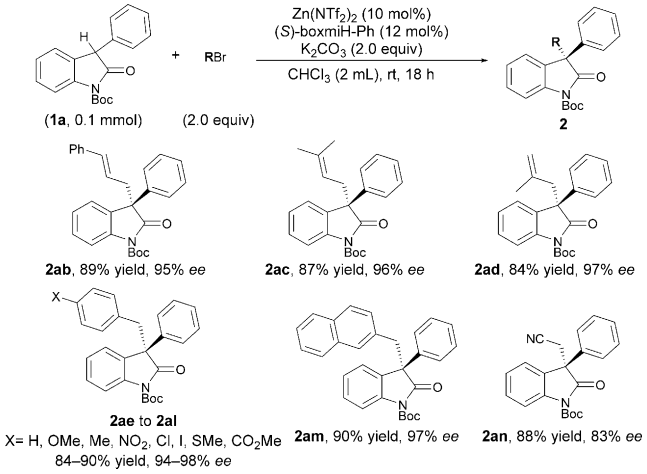

Scheme 5. Enantioselective alkylation of 3-monosubstituted oxindoles with various RBr. Yields refer to isolated products; the *ee* values were determined by HPLC analysis on a chiral stationary phase. For details on the products **2ae** to **2al**, see the Supporting Information.

products **2ab**–**2am** in high yields and excellent enantioselectivities (94–98% *ee*).

The utility of this synthetic method was demonstrated by the synthesis of the optically pure oxindole derivative **7**, which is an MDM2 inhibitor and exhibits high antitumor activity (Scheme 6).[47,48] Alkylation of oxindole **1n** with *meta*-chlorobenzyl bromide was conducted with the in situ generated ((*S*)-boxmi-Ph)Zn catalyst, and subsequent removal of the Boc group by treatment with trifluoroacetic acid afforded the corresponding product (*R*)-**7** in 96% *ee* (87% yield).

In conclusion, we have demonstrated how the specific interplay between the properties of substrates and chosen metal catalysts may lead to drastically disparate results. Understanding the mechanistic basis enabled us to develop a synthetically useful method using zinc(II) Lewis acid catalysts for the alkylation of 3-monosubstituted oxindoles,

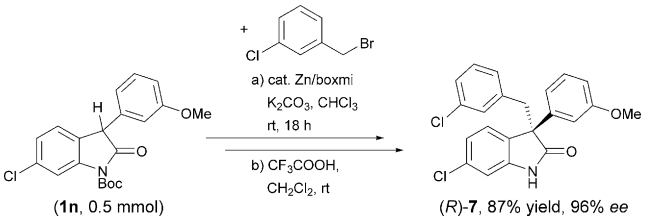

Scheme 6. Catalytic asymmetric synthesis of (*R*)-**7**.

which yielded the 3,3-dialkylated products in high yields and enantioselectivities of up to 99% *ee*. The insight gained in this study may lead to more rational catalyst design for these types of transformations.

Acknowledgements

We acknowledge funding from the Deutsche Forschungsgemeinschaft (DFG, Ga488/9-1). T.B. is grateful to the Fonds der Chemischen Industrie for a Kekulé fellowship and the Studienstiftung des Deutschen Volkes for a doctoral fellowship. We thank the bwHPC initiative (especially the JUSTUS HPC facility at Ulm University) for providing computational resources.

Keywords: copper · enantioselective catalysis · radical reactions · reaction mechanisms · zinc

How to cite: *Angew. Chem. Int. Ed.* **2016**, *55*, 7852–7856
Angew. Chem. **2016**, *128*, 7983–7987

[1] M. Bartók, *Chem. Rev.* **2010**, *110*, 1663–1705.
[2] R. Rasappan, D. Laventine, O. Reiser, *Coord. Chem. Rev.* **2008**, *252*, 702–714.
[3] M. P. Sibi, M. Liu, *Curr. Org. Chem.* **2001**, *5*, 719–755.
[4] *Copper-Catalyzed Asymmetric Synthesis* (Eds.: A. Alexakis, N. Krause, S. Woodward), Wiley, Hoboken, **2013**.
[5] M. P. Sibi, G. R. Cook in *Lewis Acids in Organic Synthesis* (Ed.: H. Yamamoto), Wiley, Hoboken, **2000**, pp. 543–574.
[6] D. Łowicki, S. Baś, J. Mlynarski, *Tetrahedron* **2015**, *71*, 1339–1394.
[7] A. P. Thankachan, S. Asha, K. S. Sindhu, G. Anilkumar, *RSC Adv.* **2015**, *5*, 62179–62193.
[8] J. Escorihuela, M. I. Burguete, S. V. Luis, *Chem. Soc. Rev.* **2013**, *42*, 5595–5617.
[9] T. Tanaka, M. Hayashi, *Synthesis* **2008**, 3361–3376.
[10] J. Li, W. Pan, Z. Wang, X. Zhang, K. Ding, *Adv. Synth. Catal.* **2012**, *354*, 1980–1986.
[11] D.-M. Du, S.-F. Lu, T. Fang, J. Xu, *J. Org. Chem.* **2005**, *70*, 3712–3715.
[12] A. Bayer, M. M. Endeshaw, O. R. Gautun, *J. Org. Chem.* **2004**, *69*, 7198–7205.
[13] N. Gathergood, W. Zhuang, K. A. Jørgensen, *J. Am. Chem. Soc.* **2000**, *122*, 12517–12522.
[14] D. A. Evans, S. J. Miller, T. Lectka, P. von Matt, *J. Am. Chem. Soc.* **1999**, *121*, 7559–7573.
[15] D. A. Evans, M. C. Kozlowski, J. S. Tedrow, *Tetrahedron Lett.* **1996**, *37*, 7481–7484.
[16] M. Çolak, T. Aral, H. Hoşgören, N. Demirel, *Tetrahedron: Asymmetry* **2007**, *18*, 1129–1133.
[17] Z.-Y. Cao, Y.-H. Wang, X.-P. Zeng, J. Zhou, *Tetrahedron Lett.* **2014**, *55*, 2571–2584.

[18] K. Shen, X. Liu, L. Lin, X. Feng, *Chem. Sci.* **2012**, *3*, 327 – 334.
[19] J. E. M. N. Klein, R. J. K. Taylor, *Eur. J. Org. Chem.* **2011**, 6821 – 6841.
[20] F. Zhou, Y.-L. Liu, J. Zhou, *Adv. Synth. Catal.* **2010**, *352*, 1381 – 1407.
[21] B. Trost, M. Brennan, *Synthesis* **2009**, 3003 – 3025.
[22] M. M. M. Santos, *Tetrahedron* **2014**, *70*, 9735 – 9757.
[23] C. V. Galliford, K. A. Scheidt, *Angew. Chem. Int. Ed.* **2007**, *46*, 8748 – 8758; *Angew. Chem.* **2007**, *119*, 8902 – 8912.
[24] M. K. Uddin, S. G. Reignier, T. Coulter, C. Montalbetti, C. Grånäs, S. Butcher, C. Krog-Jensen, J. Felding, *Bioorg. Med. Chem. Lett.* **2007**, *17*, 2854 – 2857.
[25] C. Marti, E. M. Carreira, *Eur. J. Org. Chem.* **2003**, 2209 – 2219.
[26] S. Ghosh, S. De, B. N. Kakde, S. Bhunia, A. Adhikary, A. Bisai, *Org. Lett.* **2012**, *14*, 5864 – 5867.
[27] D. Katayev, E. P. Kündig, *Helv. Chim. Acta* **2012**, *95*, 2287 – 2295.
[28] L. Liu, N. Ishida, S. Ashida, M. Murakami, *Org. Lett.* **2011**, *13*, 1666 – 1669.
[29] B. M. Trost, J. T. Masters, A. C. Burns, *Angew. Chem. Int. Ed.* **2013**, *52*, 2260 – 2264; *Angew. Chem.* **2013**, *125*, 2316 – 2320.
[30] B. M. Trost, M. Osipov, *Angew. Chem. Int. Ed.* **2013**, *52*, 9176 – 9181; *Angew. Chem.* **2013**, *125*, 9346 – 9351.
[31] C. Jing, D. Xing, W. Hu, *Org. Lett.* **2015**, *17*, 4336 – 4339.
[32] Y. Kato, M. Furutachi, Z. Chen, H. Mitsunuma, S. Matsunaga, M. Shibasaki, *J. Am. Chem. Soc.* **2009**, *131*, 9168 – 9169.
[33] L. Chen, Y. You, M.-L. Zhang, J. Zhao, J. Zuo, X.-M. Zhang, W.-C. Yuan, X.-Y. Xu, *Org. Biomol. Chem.* **2015**, *13*, 4413 – 4417.
[34] M.-X. Zhao, T.-L. Dai, R. Liu, D.-K. Wei, H. Zhou, F.-H. Ji, M. Shi, *Org. Biomol. Chem.* **2012**, *10*, 7970 – 7979.
[35] C. Wang, X. Yang, D. Enders, *Chem. Eur. J.* **2012**, *18*, 4832 – 4835.
[36] S.-W. Duan, J. An, J.-R. Chen, W.-J. Xiao, *Org. Lett.* **2011**, *13*, 2290 – 2293.
[37] N. Shibata, J. Kohno, K. Takai, T. Ishimaru, S. Nakamura, T. Toru, S. Kanemasa, *Angew. Chem. Int. Ed.* **2005**, *44*, 4204 – 4207; *Angew. Chem.* **2005**, *117*, 4276 – 4279.
[38] T. Ishimaru, N. Shibata, J. Nagai, S. Nakamura, T. Toru, S. Kanemasa, *J. Am. Chem. Soc.* **2006**, *128*, 16488 – 16489.
[39] Q.-H. Deng, H. Wadepohl, L. H. Gade, *Chem. Eur. J.* **2011**, *17*, 14922 – 14928.
[40] Q.-H. Deng, T. Bleith, H. Wadepohl, L. H. Gade, *J. Am. Chem. Soc.* **2013**, *135*, 5356 – 5359.
[41] Q.-H. Deng, H. Wadepohl, L. H. Gade, *J. Am. Chem. Soc.* **2012**, *134*, 2946 – 2949.
[42] N. Zhang, S. R. Samanta, B. M. Rosen, V. Percec, *Chem. Rev.* **2014**, *114*, 5848 – 5958.
[43] A. E. Wendlandt, A. M. Suess, S. S. Stahl, *Angew. Chem. Int. Ed.* **2011**, *50*, 11062 – 11087; *Angew. Chem.* **2011**, *123*, 11256 – 11283.
[44] M. P. DeMartino, K. Chen, P. S. Baran, *J. Am. Chem. Soc.* **2008**, *130*, 11546 – 11560.
[45] P. S. Baran, J. M. Richter, *J. Am. Chem. Soc.* **2004**, *126*, 7450 – 7451.
[46] B. M. Rosen, V. Percec, *Chem. Rev.* **2009**, *109*, 5069 – 5119.
[47] "Oxindole Derivatives": K.-C. Luk, S.-S. So, J. Zhang, Z. Zhang, WO2006136606 (A2), **2006**.
[48] S. Shangary, S. Wang, *Annu. Rev. Pharmacol. Toxicol.* **2009**, *49*, 223 – 241.

Received: March 29, 2016
Published online: June 2, 2016

